Available online at www.sciencedirect.com
ScienceDirect
Journal of Hazardous Materials 151 (2008) 585–593
Journal of Hazardous Materials
www.elsevier.com/locate/jhazmat

Reuse of cement-solidified municipal incinerator fly ash in cement mortars: Physico-mechanical and leaching characteristics

Maria Anna Cinquepalmi [a], Teresa Mangialardi [a,*], Liliana Panei [b], Antonio Evangelista Paolini [a], Luigi Piga [a]

[a] *Facoltà di Ingegneria, Università di Roma "La Sapienza", via Eudossiana, 18-00184 Roma, Italy*
[b] *Ufficio Chimico DGERM-Ministero dello Sviluppo Economico, Roma, Italy*

Received 24 January 2007; received in revised form 6 June 2007; accepted 7 June 2007
Available online 12 June 2007

Abstract

The reuse of cement-solidified Municipal Solid Waste Incinerator (MSWI) fly ash (solidified/stabilised (S/S) product) as an artificial aggregate in Portland cement mortars was investigated. The S/S product consisted of a mixture of 48 wt.% washed MSWI fly ash, 20 wt.% Portland cement and 32 wt.% water, aged for 365 days at 20 °C and 100% RH. Cement mortars (water/cement weight ratio = 0.62) were made with Portland cement, S/S product and natural sand at three replacement levels of sand with S/S product (0%, 10% and 50% by mass). After 28 days of curing at 20 °C and 100% RH, the mortar specimens were characterised for their physico-mechanical (porosity, compressive strength) and leaching behaviour. No retardation in strength development, relatively high compressive strengths (up to 36 N/mm^2) and low leaching rates of heavy metals (Cr, Cu, Pb and Zn) were always recorded. The leaching data from sequential leach tests on monolithic specimens were successfully elaborated with a pseudo-diffusional model including a chemical retardation factor related to the partial dissolution of contaminant.

Keywords: Municipal incinerator fly ash; S/S product; Reuse; Cement mortar; Heavy metals leaching; Leaching kinetic model

1. Introduction

Incineration is an increasingly adopted technology for the disposal of Municipal Solid Waste (MSW). Such a technology produces solid residues composed of bottom ash, fly ash and scrubber residue. Fly ash represents about 3% by mass of the unburned MSW and is regarded as a hazardous waste due to its high concentration of leachable heavy metals and, in some cases, to the presence of toxic chlorinated compounds [1].

Generally, municipal incinerator fly ash, also referred to as MSWI fly ash, is landfilled after a preliminary treatment such as advanced separation processes, chemical stabilisation or encapsulation, solidification/stabilisation with inorganic binders (cement, powdered blast furnace slag or calcium sulphate) [1–3]. Such a pre-treatment is needed in order to reduce the hazardous characteristics of MSWI fly ash.

Cement solidification/stabilisation is certainly one of the most popular techniques but there are strong limitations regarding the amount of raw MSWI fly ash that can be incorporated into cementitious mixes. This is related to the adverse effects of the chemical composition of raw MSWI fly ash (high contents of chlorides, sulphates and heavy metals) on the hydration of cement and the stability of solidified/stabilised (S/S) products [4–6].

As reported in previous works [5,7] aimed at maximising the incorporation of MSWI fly ash into cementitious mixes for landfill disposal purposes, a preliminary washing treatment of raw fly ash with water followed by cement stabilisation is a suitable way of obtaining S/S products with high ash content and good performance characteristics. Reuse of such products in place of their landfill disposal is clearly the preferable option.

Our recent studies [8,9] have shown that using S/S product as an artificial aggregate in cement mortars may represent a sensible method of safe reuse of MSWI fly ash (reduction of environmental problems and costs associated with both land disposal and irreplaceable natural resources utilisation). However, in such studies it was found that the mechanical strength

* Corresponding author. Tel.: +39 06 44 58 55 75; fax: +39 06 44 58 54 51.
E-mail address: teresa.mangialardi@ingchim.ing.uniroma1.it (T. Mangialardi).

0304-3894/$ – see front matter © 2007 Elsevier B.V. All rights reserved.
doi:10.1016/j.jhazmat.2007.06.026

development for mortars incorporating artificial aggregate was somewhat penalized by the lower compressive strength of S/S product as compared to cement paste. Moreover, a deeper knowledge about the mechanisms of immobilisation of heavy metals by the two components of the artificial aggregate-incorporating mortars (S/S product and cement paste) would be desirable for a better prediction of the long-term leaching behaviour of such mortars.

In the present study, Portland cement mortars made with different amounts of an older S/S product characterised by higher compressive strength were investigated for their physico-mechanical and leaching behaviour. The leaching data for selected heavy metals (Cr, Cu, Pb and Zn) obtained from sequential monolith leach tests were also elaborated with a pseudo-diffusional leaching model in order to identify the release mechanisms of such heavy metals and to predict the long-term leaching behaviour of cement mortars.

2. Development of pseudo-diffusional leaching model

A simple leaching kinetic model was developed to correlate the time-dependent release of heavy metals from monolithic mortar specimens when subjected to sequential leach tests.

This model was based on a one-dimensional Fickian diffusion equation (zero surface concentration at the solid–liquid interface and associated zero leachant concentration) [10], that was appositely modified to include a release retardation factor related to the partial dissolution (partial availability) of the contaminant of interest (heavy metal, in the present study) within the pore solution of the cementitious matrix.

According to this model, the cumulative mass of contaminant released per unit exposed surface area of monolithic specimen, M_t (mg/m^2), may be related to the leach time, t (s), through the equation:

$$M_t = 2 f_{av} C_0 \sqrt{\frac{D_e t}{\pi}} \quad (1)$$

where f_{av} is the leachable (or mobile) fraction of contaminant within the monolithic specimen, also referred to as the availability or chemical retardation factor (dimensionless), C_0 (mg/m^3) the total (bulk) concentration of contaminant within the monolithic specimen and D_e (m^2/s) is the effective diffusion coefficient of the contaminant. The chemical retardation factor, f_{av}, includes all chemical reactions (dissolution, precipitation, ion exchange, sorption, complexation) affecting the leaching rate of the chemical species of concern.

The effective diffusion coefficient, D_e, of the contaminant is related to its molecular diffusion coefficient, D_0 (m^2/s), by a geometric factor that is characteristic of the porous medium. If the pore geometry is unknown, the geometric factor, Φ, is usually defined in terms of two parameters, the solid porosity, ε (m^3/m^3) and the tortuosity factor, τ [11,12], and D_e may be calculated as:

$$D_e = \frac{D_0 \varepsilon}{\tau} = D_0 \Phi \quad (2)$$

where Φ is defined by the term ε/τ and is also known as physical retention factor. The tortuosity factor, τ, may vary from values of less than unity (significant surface diffusion) to more than 6 [12]. Moreover, in the case of porous solids characterised by a significant presence of micropores (pore radius <1 nm) [13], Φ should also include a steric hindrance factor, β (<1), to take into account the reduction of diffusivity due to hindered diffusion. Thus, according to Eq. (2), higher Φ values will denote lower physical retention capabilities of contaminant by solid matrices.

The concentration C_0' (mg/m^3) of contaminant dissolved within the pore solution of the monolithic specimen (leachable or mobile concentration) is related to its total concentration, C_0, by the equation:

$$C_0' = \frac{f_{av} C_0}{\varepsilon} \quad (3)$$

In the present study, the physical retention factors, Φ, of the solid matrices were estimated from the leaching data of sodium ions and the availability factors, f_{av}, of this species, the latter being calculated according to the test procedure developed by Kosson et al. [14].

Thus, the pseudo-diffusional model developed in this study represents an alternative approach to the commonly adopted pure diffusive model using an observed (apparent) diffusion coefficient, D_{obs}, that includes all physical and chemical factors affecting leaching rates [15].

3. Materials and methods

The S/S product tested as an artificial aggregate (AA) for use in cement mortars came from a laboratory-scale solidification/stabilisation process of washed MSWI fly ash with Portland cement (CEM I 42.5), after a preliminary four-stage washing treatment of raw fly ash with deionised water (liquid-to-solid weight ratio of 12.5 and contact time of 30 min for each washing step). The physico-chemical and mineralogical characterisation of raw and washed MSWI fly ash, as well as the analysis of the washing process and cement-stabilisation treatment of washed MSWI fly ash have been reported in previous papers [7,8,16].

The S/S product (washed MSWI fly ash-to-cement weight ratio = 70:30; water-to-solid weight ratio = 0.47) tested here had a curing time of 365 days at 20 °C and 100% relative humidity (RH) and was characterised by an average compressive strength, R_c, of 32 N/mm^2, against 27 N/mm^2 for the same S/S product aged for 180 days and used in our previous studies [8,9].

The S/S product was ground to a size grading (particle sizes ranging from 0.08 to 2.0 mm) closely resembling that of natural sand, and was then analysed for its chemical composition and physical properties according to standard test procedures. Table 1 gives the chemical and physical characteristics of the S/S product (artificial aggregate) together with those of the Portland cement (CEM I 52.5) used to prepare mortar samples.

A quartzitic sand (SiO_2 = 91.2%; Na_2O = 0.80%; K_2O = 0.72%; particle density = 2.65 g/cm^3; water absorption = 0.80%; size gradation = 0.08–2.00 mm), virtually free of heavy metals such as Cr, Cu, Pb and Zn [8], was used to prepare

Table 1
Chemical and physical characteristics of Portland cement and S/S product

Component (%)	Portland cement[a]	S/S product	Component (mg/kg)	Portland cement[a]	S/S product
CaO	61.97	25.96	Cr	38	118
SiO_2	20.02	18.71	Cu	30	590
Fe_2O_3	2.94	1.65	Pb	120	2,500
Al_2O_3	4.26	8.20	Zn	160	4,500
MgO	1.36	1.78	L.O.I. (950 °C) (%)	1.20	37.51
SO_3	2.99	2.09	Bulk specific gravity	3.15	1.83
Na_2O	0.23	0.88	Specific surface area (m^2/kg)	500	23,300
K_2O	1.40	0.11		Blaine	Mercury porosimetry
Cl	0.01	0.02			

[a] Bogue potential constituents: $C_3S = 55.80\%$; $C_2S = 15.32\%$; $C_3A = 6.32\%$; $C_4AF = 8.95\%$.

blends with artificial aggregate at sand replacement levels of 0% (control), 10% and 50% by mass.

Mortar samples were made by mixing Portland cement, dry aggregate (natural sand and artificial aggregate) and deionised water at a nominal water-to-cement weight ratio of 0.62 and a total aggregate-to-cement weight ratio of 3.0. For all mortars incorporating artificial aggregate, a sulphonated naphthalene-based superplasticiser at a dose level of 2.0 wt.% of cement was used to improve mix workability.

Each mixture was used to prepare prismatic and cubic specimens for compressive strength measurements and leaching tests, respectively. After the 1-day storage of the mortar specimens in the moulds at ambient temperature and RH > 90%, these specimens were demoulded and transferred to the moist-curing room at 20 °C and 100% RH, until required for testing.

Compressive strength was periodically measured up to 90 days of curing on three replicate 40 mm × 40 mm × 160 mm specimens.

After 28 days of curing, all mortar specimens were also characterised for their porosity, pore size distribution and heavy metals leachability.

The porosity and the pore size distribution were measured on broken prismatic specimens through the use of a mercury intrusion porosimeter operating at a maximum pressure of 2000 atm, corresponding to a cylindrical pore radius of about 3.8 nm.

The heavy metals leachability was evaluated using the standard CEN/TS 14429 pH-dependence leaching test [17] and a modified version of the sequential monolith leach test developed by Kosson et al. [14].

The pH-dependence leaching test was performed on crushed mortar samples (particle sizes <1.0 mm). Ten-gram samples were mixed with aqueous solutions having different concentrations of nitric acid. The slurries, having a liquid-to-solid ratio (L/S) of 10 cm^3/g dry matter, were mixed for 48 h in a rotary extractor and then centrifuged at 4000 rpm for 10 min. Each leachate was extracted and, after pH measurement, was filtered through a 0.45 μm membrane filter, acidified with 1 M HNO_3 to pH 2.0, and finally analysed for the selected heavy metals (Cr, Cu, Pb and Zn). The heavy metals concentrations were determined using an atomic absorption spectrophotometer (AAS) equipped with a graphite furnace.

The sequential monolith leach test was performed using three 40 mm cubic specimens of the same mortar mix that were placed in a sealed tank and contacted with the leachant. Deionised water (initial pH of 4.0 through addition of nitric acid) was used as a leachant and the leachant volume-to-solid surface area ratio was 10 cm^3/cm^2, corresponding to an L/S volume ratio of 15.0. The leachate was removed and replaced with an equal volume of leachant after cumulative leach times of 2, 5, 8, 24, 48, 96 and 192 h. In order to better evaluate the leaching of heavy metals from mortar specimens, the leach test was modified by prolonging the test duration from 192 h to 64 days, with three intermediate renewals of leachant after cumulative times of 14, 21 and 34 days. Each leachate was analysed for the selected heavy metals and sodium according to the same procedure as described for the pH-dependence leach test.

The availability factor, f_{av}, of sodium ions in the pore water of each solid matrix was estimated using the test procedure developed by Kosson et al. [14]. This procedure consisted of performing parallel extractions with deionised water at different L/S ratios (10, 5, 2, 1 and 0.6 cm^3/g of dry solid). For each extraction, an aliquot of finely crushed dry mortar (<125 μm) was contacted with deionised water for 48 h at ambient temperature. The liquid phase was then separated by centrifugation and analysed for sodium concentration by using AAS. The sodium concentrations thus obtained were correlated with the L/S ratio as discussed later.

4. Results and discussion

4.1. Physico-mechanical characteristics of cement mortars

Figs. 1 and 2 show, respectively, the effects of partially replacing natural sand with S/S product on the mercury intrusion porosity and the pore size distribution of the various types of mortar aged for 28 days at 20 °C and 100% RH. In these two figures, the total porosity and the pore size distribution of the artificial aggregate used for the preparation of mortar samples are also reported.

It must be emphasized that, for simplicity, the results of the mercury intrusion porosimetry are labelled as "total porosity" in the present paper, although this technique is not able to determine pores with radius smaller than 3.8 nm.

In cement-based materials, such pores are included in the volume occupied by hydrated cement constituents (silicates and aluminates) and they represent a relevant proportion of the

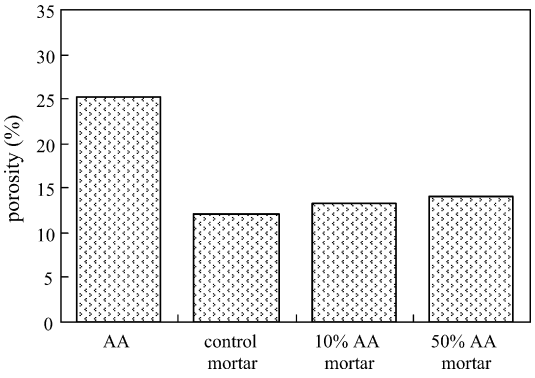

Fig. 1. Mercury intrusion porosity of artificial aggregate and cement mortars.

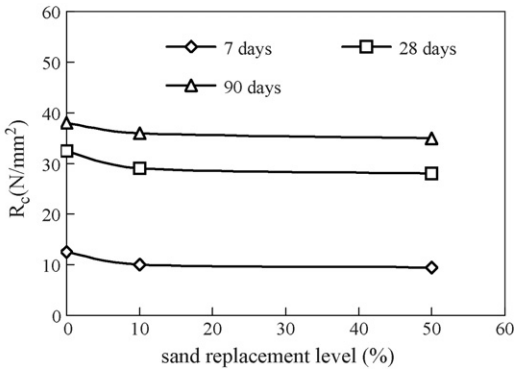

Fig. 3. Development of compressive strength for control and artificial aggregate-incorporating mortars.

cement gel pores (pore radii smaller than 5 nm). However, gel pores are reported to give a negligible contribution to leaching [18,19].

The data in Fig. 1 revealed that there was no significant difference between the mercury intrusion porosities of the control and artificial aggregate-incorporating mortars: the total porosity ranged from 12.2% (control mortar) to 13.3% and 14.0% for 10% AA- and 50% AA-incorporating mortars, respectively. This was in spite of the much higher porosity of the artificial aggregate (25.2%) as compared to both natural sand (about 2.0% from water absorption measurement) and control mortar (12.2%).

A possible explanation of these results could be related to coating of artificial aggregate with hydrated cement paste. In that case, the porosity of the various types of mortar would be largely determined by the porosity of the hydrated cement paste within the mortar samples. However, it must be considered that: (1) at a fixed nominal water/cement ratio (w/c = 0.62), an increase of the replacement level of natural sand with artificial aggregate results in a significant reduction of the actual w/c ratio (free water-to-cement ratio), as a consequence of the much higher water absorption exhibited by artificial aggregate (about 14.6% as estimated from its density (Table 1) and porosity (Fig. 1), against 0.80% for natural sand), (2) the capillary porosity of the hydrated cement paste within the mortars is expected to markedly reduce with decreasing actual w/c ratio [18] and (3) water absorption by aggregate always precedes eventual coating by hydrated cement paste.

Thus, the porosimetric data in Fig. 1 could not be explained by the only coating phenomenon: complete coating of artificial aggregate with cement paste would lead to a significant reduction in the porosity of mortars incorporating S/S product, as compared to control mortar. Therefore, the reduction in the actual w/c ratio of cement paste with increasing amount of artificial aggregate should be considered the predominant mechanism affecting the porosity of mortars incorporating artificial aggregate. These argumentations were validated by the similar pore size distribution curves exhibited by the artificial aggregate and 50% AA-incorporating mortar, as well as by the relative position of the curves showing the pore size distributions of control and 10% AA-incorporating mortar (Fig. 2).

The curves of Fig. 2 also showed that the artificial aggregate was characterised by the same overall pore size interval as that of the control mortar, but it was more rich in smaller pores over the whole range of pore sizes explored by mercury intrusion porosimetry (pore radius from 3.8 to 6800 nm).

The frequency distribution of discrete pore size intervals (not reported here) showed that, irrespective of the solid considered (artificial aggregate or cement mortar), the largest volume percentage of pores (24–41%) always fell within the 10–25 nm pore radius interval, that is near the upper size limit of mesopores (1 nm ≤ pore radius ≤ 25 nm) [13]. Also, the volume percentage of macropores (pore radius > 25 nm) varied from about 33% (artificial aggregate) to 51% (control mortar), with about 14% of total porosity formed by macropores with radii larger than 250 nm (Fig. 2). The formation of macropores was mainly associated to the interfacial transition zones occurring between aggregate and hydrated cement particles.

Fig. 3 shows the effect of increasing the sand replacement level on the compressive strength of the various types of mortar after 7, 28 and 90 days of curing at 20 °C and 100% RH.

Within the range of sand replacement levels investigated (0–50% by mass), no delay in the strength development was observed and only a slight reduction in the compressive strength (4–7%) was recorded as natural sand was partially replaced by artificial aggregate. At 90 days of curing, relatively high average R_c values were measured: 38 N/mm^2 for control mortar, 36 and 35 N/mm^2 for 10% AA- and 50% AA-incorporating mortars,

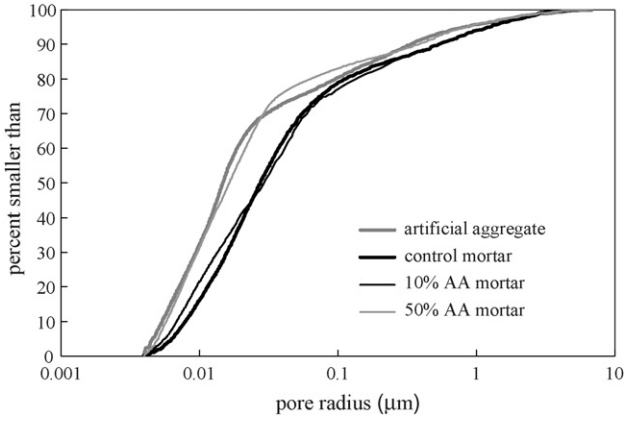

Fig. 2. Pore size distribution of artificial aggregate and cement mortars.

respectively. These results were consistent with the comparable porosities exhibited by the various types of mortar investigated (Fig. 1) and also indicated that the artificial aggregate behaved as an almost inert material. In other words, the S/S product used as an artificial aggregate did not negatively interfere with cement hydration kinetics (possible retarding effect) and strength development.

It was also noteworthy that, after 90 days of curing, the mortars incorporating artificial aggregate exhibited R_c values that were somewhat higher than the compressive strength (32 N/mm^2) of the artificial aggregate used for mortar preparation. This result was attributable to an improvement in the compressive strength of the artificial aggregate during mortar curing as a result of its chemical interaction with Portland cement.

4.2. Leaching characteristics of crushed mortar samples

Fig. 4 shows the results of the standard pH-dependence leach test on crushed samples of the various types of mortar investigated. In this figure, the release of each heavy metal, expressed in terms of mass of metal leached per unit mass of dry solid, m_s (mg/kg), is plotted as a function of final leachate pH. The total metal concentration, m_0 (mg/kg), determined by $HNO_3/HClO_4/HF$ digestion of pulverised mortar samples, is also reported as a horizontal line.

The results in Fig. 4 proved the great influence of pH on the leachability of heavy metals from the various types of mortar.

At pH values above 6–8, depending on the heavy metal examined, the release, m_s, was found to be very low and virtually unaffected by the amount of artificial aggregate present in the mortar specimens. This fact could be ascribed to a metal release mechanism governed by the solubility of the same metal compound present within the cement paste and the artificial aggregate. Another possible explanation could be no significant contribution by the artificial aggregate to the amount of heavy metal released from the cement paste present within the mortar specimens. In every case, the various types of mortar showed similar leaching behaviour with regard to a specific heavy metal.

Conversely, at pH values below 6–8, depending on the heavy metal examined, a remarkable increase in the metal release was observed for each type of mortar. Also, the release of each metal greatly increased with increasing amount of artificial aggregate in the mortar specimens. In the case of the control mortar (absence of artificial aggregate), a pH value of less than 2.0 was able to produce a release of the examined heavy metal that broadly approached its total concentration, m_0, in the mortar. Conversely, in the case of mortars incorporating artificial aggregate, even at the lowest pHs tested in this study (pH 1.1 and 2.0 for mortars incorporating 10% AA and 50% AA, respectively), the leaching of the examined heavy metals resulted to be rather incomplete ($m_s < m_0$). Thus, the leaching data at low-medium pHs suggested that the heavy metals present within the artificial aggregate were much more retained than the same species present within Portland cement.

4.3. Leaching characteristics of monolithic mortar specimens

Fig. 5 shows the changes in the pH of leachant during each leaching interval when monolithic specimens of control mortar (aged for 28 days at 20 °C and 100% RH) were subjected to sequential leach test (10 leachant renewals) with deionised water (initial pH 4.0). The leachant pH–time plots for mortars incorporating artificial aggregate (not reported here) did not differ significantly from that of control mortar.

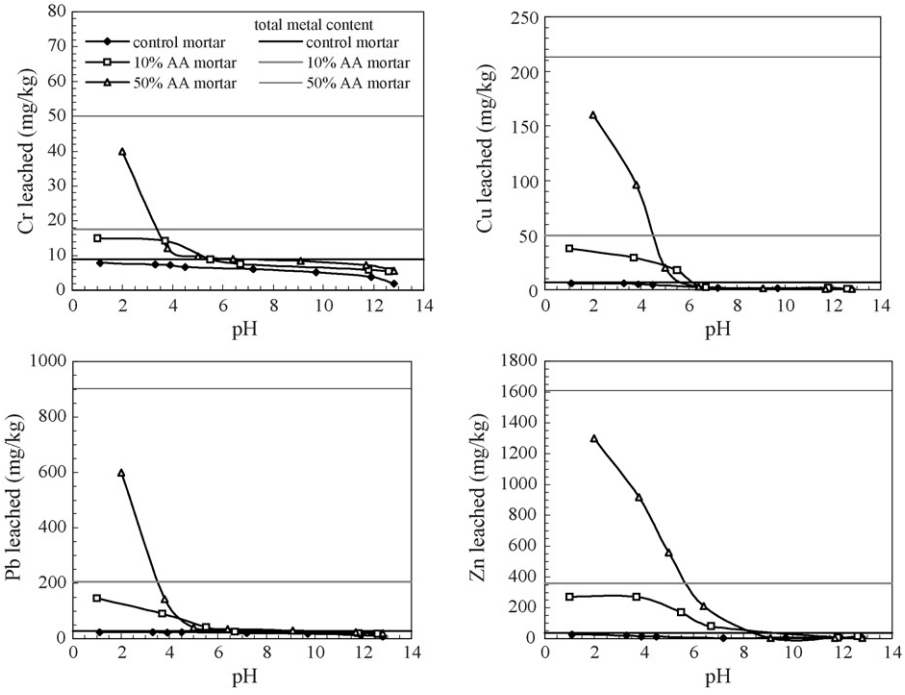

Fig. 4. Results of pH-dependence leach test on the various types of mortar investigated.

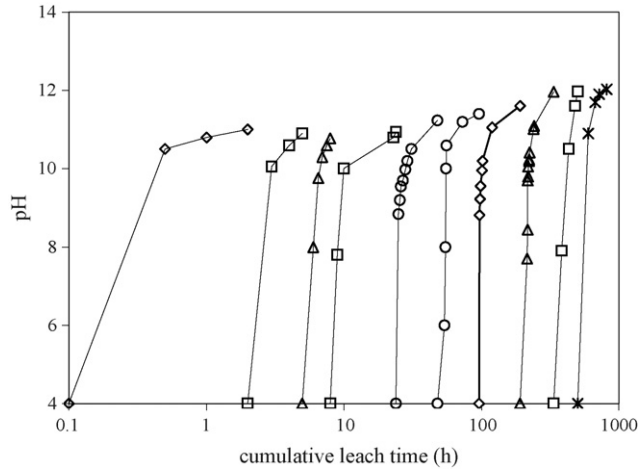

Fig. 5. Evolution of leachant pH during sequential monolith leach test.

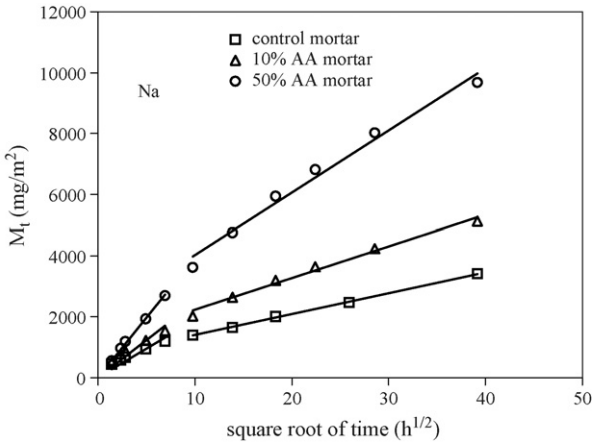

Fig. 7. Results of sequential monolith leach test on the various types of mortar: sodium release.

The pH measurements revealed that, after 1–4 h of leaching, the pH of the leachant was always above 10 during each leaching interval and the final pH resulted to be over the range from 10.9 to 12.0, depending on the duration of the leaching interval and its location in the renewals sequence.

The rapid pH increases as well as the high final pHs of the leachates were related to a rapid release of alkalies (principally those coming from Portland cement) and portlandite (mainly resulting from the hydration of cement silicate constituents) from mortar specimens. The weighted average pH of the overall leaching test was calculated to be 11.4 for control mortar, 11.8 and 11.7 for 10% AA- and 50% AA-incorporating mortars, respectively.

Figs. 6 and 7 show, respectively, the releases of the selected heavy metals (Cr, Cu, Pb and Zn) and sodium from the monolithic mortar specimens when subjected to the sequential leach test. In these figures, the cumulative mass of each metal released per unit exposed surface area of specimen, M_t (mg/m^2), is plotted against the square root of leach time, t (h$^{1/2}$).

As far as the leaching of heavy metals was concerned, the results of Fig. 6 revealed that: (1) irrespective of the type of mortar and heavy metal examined, each release curve was always characterised by two distinct linear parts, both indicating a square root of time linear dependence of the cumulative release, M_t; (2) irrespective of the heavy metal examined, the changes in the slope of the release curves always occurred after a cumulative leach time of between 48 and 96 h (i.e., after the fourth leachant renewal), thus suggesting that the slope variation was mainly related to the physical properties of the solid matrices; (3) after the early leaching phase characterised by higher leaching rates, the release of each heavy metal was always low (especially in the case of Cr, Cu and Pb), at least up to the ultimate leaching time investigated (64 days); (4) there was no remarkable difference between the releases of a specific metal from the various types of mortar examined. Indeed, the metal release from the control mortar was always slightly higher than that measured for the artificial aggregate-incorporating mortars, and this was in spite of the much higher metal content of artificial aggregate as compared to cement paste (Table 1); (5) irrespective of the type of mortar examined, the highest leaching rates were always recorded for Zn (predominant heavy metal), while the lowest release rates were always measured for Cr (lowest C_0 values).

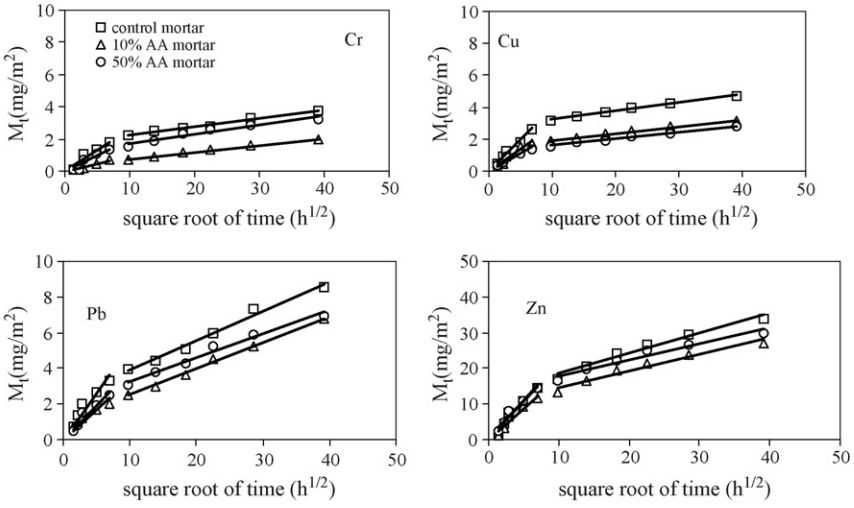

Fig. 6. Results of sequential monolith leach test on the various types of mortar: heavy metals release.

Considering that the various types of mortar differed remarkably for the total metal concentration, m_0 (Fig. 4) but only slightly for their total porosity (Fig. 1) and pore size distribution (Fig. 2), it was likely to think that the observed releases, M_t, of a given metal (Fig. 6) were strongly dependent on the porous structures of the solid matrices and poorly affected by the total concentration of heavy metal.

As far as the leaching of sodium was concerned (Fig. 7), relatively high leaching rates were always recorded and each release curve was characterised by two distinct portions, thus confirming that the slope variation was mainly related to the physical properties of the solid matrices. Differently from what was observed for the leaching of heavy metals, the release of sodium ions increased remarkably with increasing amount of artificial aggregate in the mortar, i.e., with increasing total content of sodium.

4.4. Correlation of monolith leaching data with the pseudo-diffusional equation

4.4.1. Leaching of sodium

For ionic species such as Na^+ ions, commonly coming from highly water-soluble compounds whose solubility is virtually independent of the leachant pH, the availability factor, f_{av}, is often taken equal to 1. However, Sanchez et al. [20] reported that, in the case of soil and S/S As_2O_3 matrices, the correlation of leaching data with a pure diffusive model using the total concentration of sodium underestimated (up to three orders of magnitude) the effective diffusion coefficient, D_e, of this species.

On the other hand, chemical analyses of the pore solution of high-alkali Portland cement mortars and concretes (w/c = 0.50) extracted by a high pressure apparatus [21–23] have shown that, after 28 days of curing, the pore solution essentially consists of OH^- (385–430 mmoles/l), Na^+ (120–130 mmoles/l), K^+ (310–330 mmoles/l), Ca^{2+} (0.36–1.4 mmoles/l) and SO_4^{2-} (10–18 mmoles/l) ions. The sodium and potassium ions are essentially released from Portland cement and no appreciable release comes from natural aggregate (siliceous sand). In particular, the release of sodium (availability factor) corresponds to about 41–45% of the total Na content of cement.

As anticipated, the test procedure developed by Kosson et al. [14] was used in this study to estimate the availability factor of sodium in the pore water of the solid matrices investigated.

Fig. 8 shows the weight fraction, F, of sodium released from each type of mortar in the leach tests with different L/S ratios. The F values were calculated from the amounts of sodium released and its total content, C_0, in each mortar.

The values of the availability factor, f_{av}, in the pore water were obtained by extrapolation of each curve to the L/S ratio equal to ε/ρ [14,20]. This ratio corresponds to the pore water L/S ratio within the matrix, and ε and ρ are, respectively, the porosity (cm^3/cm^3) and the dry density (g/cm^3) of the unleached solid matrix (ρ = 2.2, 2.1 and 2.0 g/cm^3 for control, 10% AA-, and 50% AA-incorporating mortars, respectively).

The f_{av} values for the control, 10% AA- and 50% AA-incorporating mortars resulted to be 0.37, 0.27 and 0.14, respectively.

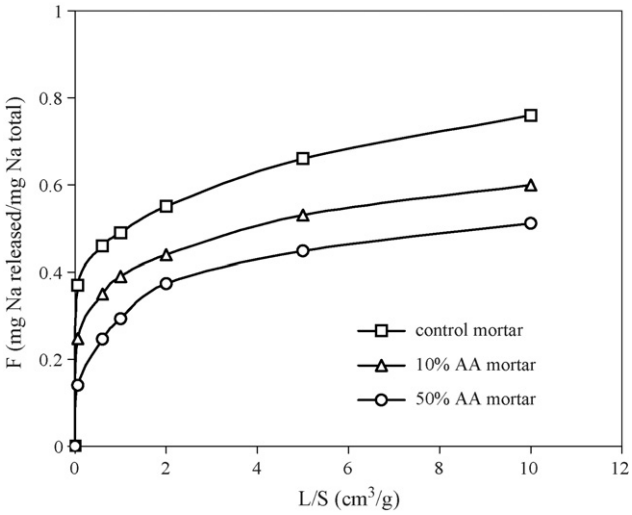

Fig. 8. Leachable fraction of sodium from the various types of mortar at different liquid-to-solid ratios.

It was noteworthy that the f_{av} value estimated for the control mortar was comparable to those (0.41–0.45) determined on Portland cement mortars and concretes through the use of the pore solution extraction technique [21–23].

Thus, the leaching data for sodium corresponding to the first and second leaching period (Fig. 7) were correlated with Eq. (1) using the total concentration, C_0, of sodium in the various types of mortar and the f_{av} values estimated from the data in Fig. 8.

Table 2 gives the values of the effective diffusion coefficient, D_e, of sodium, in terms of $pD_e = -\log D_e$, for the two leaching periods considered. The values of D_{e1} and D_{e2} thus obtained were then used to calculate the physical retention factors (Φ_1 and Φ_2) and the tortuosity factors (τ_1 and τ_2) by using Eq. (2). The D_0 value of 1.26×10^{-9} m^2/s [24] was used for sodium in Eq. (2). The values of Φ and τ thus calculated are reported in Table 2.

The values of D_e, Φ and τ were consistent with the pore structures of the solid matrices investigated (45–51% of macropores, with about 14% of total porosity formed by pores with radius >250 nm (megapores)). In particular, the early leaching of sodium was characterised by pD_{e1} values (10.0–10.2) that were indicative of a metal diffusion through the large defects (megapores) and, in part, macropores of the solid matrices. The subsequent leaching phase, characterised by higher values of pD_e (pD_{e2} = 10.8–11.0), was associated to a metal diffusion through macropores and, to a minor extent, through mesopores.

For each leaching period, the physical retention factor (Φ_1 or Φ_2) and, hence, the effective diffusion coefficient (D_{e1} or D_{e2}) were very little affected by the type of mortar, and this was consistent with the similar porosities and pore size distributions exhibited by the mortars investigated (Figs. 1 and 2).

The values of τ_2 were always found to be much higher than τ_1 values and this was ascribed to a finer pore structure involved with the diffusion process during the second leaching period. The average τ_2/τ_1 ratio (5.7) was approximately equal to the ratio calculated assuming τ_2 and τ_1 to be proportional to the

Table 2
Diffusion parameters for sodium ions in the various types of mortar investigated

Mortar (% AA)	pD_0	pD_{e1}	pD_{e2}	Φ_1	Φ_2	τ_1	τ_2	τ_2/τ_1
0	8.90	10.06	10.95	0.070	0.009	1.75	13.6	7.7
10	8.90	10.19	10.95	0.051	0.009	2.57	14.4	5.6
50	8.90	10.17	10.74	0.054	0.014	2.61	10.0	3.8

Table 3
Diffusion coefficients, availability factors and leachable concentrations for each type of heavy metal and mortar investigated

Heavy metal	Mortar (% AA)	pD_0	pD_{e1}	pD_{e2}	pf_{av1}	pf_{av2}	C'_{01} (mg/l)	C'_{02} (mg/l)
	0	8.90	10.05	10.95	1.68	1.90	3.33	1.94
Cr	10	8.90	10.19	10.95	2.34	2.30	1.25	1.39
	50	8.90	10.17	10.75	2.46	2.67	2.46	1.51
	0	9.10	10.25	11.15	1.51	1.75	3.80	2.17
Cu	10	9.10	10.39	11.15	2.22	2.65	4.71	1.74
	50	9.10	10.38	11.95	2.94	3.36	3.48	1.33
	0	9.00	10.15	11.05	1.88	1.92	7.55	6.78
Pb	10	9.00	10.29	11.05	2.80	2.83	5.13	4.89
	50	9.00	10.27	10.85	3.37	3.48	5.51	4.23
	0	9.20	10.35	11.25	1.24	1.46	39.2	23.8
Zn	10	9.20	10.49	11.25	2.22	2.43	34.5	21.2
	50	9.20	10.47	11.05	2.76	3.16	39.6	16.0

volume percentages of macropores plus mesopores (about 86% on total) and megapores (about 14%), respectively.

4.4.2. Leaching of heavy metals

On the basis of the range of solid pore sizes involved with the diffusive process during both leaching periods, the physical retention factor, Φ, was assumed to be independent of the type of diffusing species. Thus, the effective diffusion coefficient, D_e, for each of the examined heavy metals was calculated using Eq. (2), the values of Φ_1 and Φ_2 given in Table 2, and the D_0 value taken from CRC Handbook [24]. Next, the leaching data of Fig. 6 were correlated with Eq. (1) using the values of D_{e1} and D_{e2}, and the experimental value of total concentration, C_0, of the heavy metal of concern. The values of f_{av1} and f_{av2} thus obtained, along with the values of the porosity, ε, measured on the various types of mortar prior to leaching, were finally used to calculate the leachable concentration C'_0 with Eq. (3). The use of ε in place of ε_{ls} (porosity of leached shell) was considered to be an acceptable approximation, taking in mind the low leaching rates of cementitious matrices (portlandite dissolution) occurring at pH 11.4–11.8 (average pHs of leachant during sequential monolith leach tests).

Table 3 gives the results of this elaboration for each heavy metal and leaching period considered.

As expected, very low f_{av} values (high pf_{av} values) were always obtained due to the very low solubility of the examined heavy metals (metal hydroxides) over the range of pHs from about 13.5 (pH of the pore water within unleached cementitious matrices [18]) to 11.4–11.8 [25,26]. The pH variation from about 13.5 to 11.4–11.8 corresponded to the pH evolution within the leached shell of the monolithic mortar specimens investigated. Thus, the availability factor, f_{av}, as calculated from Eq. (1), included the effect of varying pH and ionic strength on the solubility of heavy metals within the pore solution of the cementitious matrices.

The f_{av} values were also found to significantly reduce with increasing amount of artificial aggregate in the mortars, as a result of a significant increase of the total content, C_0, of the heavy metal of concern.

Irrespective of the type of mortar and heavy metal considered, a slight reduction in the availability factor was systematically observed after the first leaching period ($pf_{av2} > pf_{av1}$). This f_{av} reduction could be ascribed to concomitant or individual causes such as: (1) reduction in the pH gradient within the leached shell of monoliths, (2) change in the leaching-controlling mechanism (after the first leaching period, the dissolution rate of the heavy metals could become the release-controlling mechanism) and (3) slight overestimate of D_{e2} (the physical retention factor, Φ, could actually be lower than that evaluated for Na ions, i.e., Φ is not independent of the type of diffusing species).

The values of C'_0 in Table 3 were broadly consistent with the solubility data reported in the literature [25,26], taking into account the effects of varying pH and ionic strength on the solubility of metal hydroxides.

5. Conclusions

The use of cement-solidified MSW incinerator fly ash as an artificial aggregate in Portland cement mortars proves to be a suitable way of safe reuse of such a waste.

No delay in mechanical strength development, relatively high compressive strengths (up to 36 N/mm^2 after 90 days of curing) and low leaching rates of heavy metals (Cr, Cu, Pb and Zn) were always recorded for the mortars incorporating

artificial aggregate (sand replacement levels of 10% and 50% by mass).

The leaching data of heavy metals from sequential leach tests on monolithic mortar specimens (deionised water as a leachant; not controlled leachant pH) may be successfully elaborated by a simple pseudo-diffusional kinetic model that includes a chemical retardation factor related to the partial dissolution of contaminant.

On the basis of the promising results of this study, there exist real possibilities of reusing S/S products as coarse aggregates in concrete formulations. This would be a more attractive application in consideration of the lower energy needed for grinding S/S products to coarser particle sizes.

References

[1] J.R. Conner, Chemical Fixation and Solidification of Hazardous Wastes, Van Nostrand-Reinhold, New York, 1990.

[2] K.Y. Cheng, P.L. Bishop, Sorption, important in stabilized/solidified waste forms, Hazard. Waste Hazard. Mater. 9 (3) (1992) 289–296.

[3] H.A. Van der Sloot, D. Hoede, D.J.F. Cresswell, J.R. Barton, Leaching behaviour of synthetic aggregates, Waste Manage. 21 (2001) 221–228.

[4] F.P. Glasser, Fundamental aspects of cement solidification and stabilisation, J. Hazard. Mater. 52 (2–3) (1997) 151–170.

[5] T. Mangialardi, A.E. Paolini, A. Polettini, P. Sirini, Optimization of the solidification/stabilization process of MSW fly ash in cementitious matrices, J. Hazard. Mater. B70 (1–2) (1999) 53–70.

[6] S. Rémond, P. Pimienta, D.P. Bentz, Effects of the incorporation of municipal solid waste incineration fly ash in cement pastes and mortars, Cem. Concr. Res. 32 (2) (2002) 303–311.

[7] T. Mangialardi, Effects of a washing pretreatment of municipal solid waste incineration fly ash on the hydration behaviour and properties of ash-Portland cement mixtures, Adv. Cem. Res. 16 (2) (2004) 45–54.

[8] T. Mangialardi, L. Panei, L. Piga, Cement-based immobilisation of municipal incinerator fly ash and reuse of solidified products as a construction material, in: Proceedings of 2nd International Conference on Waste Management and the Environment, Rodhes, 29 September–1 October, 2004, pp. 35–44.

[9] T. Mangialardi, L. Panei, A.E. Paolini, L. Piga, Recycling of municipal incinerator fly ash into cementitious mixes through a preliminary solidification/stabilisation process, in: Proc. World Environment Congress and Exhibition ISWA 2004, Rome, 17–21 October, 2004, CD-ROM.

[10] American Nuclear Society, Measurement of the leachability of solidified low-level radioactive wastes by a short-term test procedure, ANSI/ANS-16.1-1986, pp. 21–35.

[11] E.E. Petersen, Chemical Reaction Analysis, Prentice-Hall Inc., Englewood Cliffs, New Jersey, 1965.

[12] J.M. Smith, Chemical Engineering Kinetics, McGraw-Hill Kogakusha Ltd., Tokyo, 1970.

[13] IUPAC, Recommendations for the characterization of porous solids, Pure Appl. Chem. 66 (1994) 1739–1758.

[14] D.S. Kosson, H.A. Van der Sloot, F. Sanchez, A.C. Garrabrants, An integrated framework for evaluating leaching in waste management and utilization of secondary materials, Environ. Eng. Sci. 19 (3) (2002) 159–204.

[15] B. Batchelor, Leach models for contaminants immobilized by pH-dependent mechanisms, Environ. Sci. Technol. 32 (1998) 1721–1726.

[16] F. Domenichini, T. Mangialardi, A.E. Paolini, Solidification/stabilisation of MSW incinerator fly ash for reuse in concrete, in: Proc. 4th Int. Congress on Added Value and Recycling of Industrial Waste, L'Aquila, 24–27 June, 2003, CD-ROM.

[17] CEN/TS 14429 Characterization of waste – leaching behaviour tests – influence of pH on leaching with initial acid–base addition, CEN, European Committee for Standardization, Brussels, 2005.

[18] H.F.W. Taylor, Cement Chemistry, Academic Press, London, 1990.

[19] D.P. Bentz, E.J. Garboczi, Modeling the leaching of calcium hydroxide from cement paste: effects on pore space percolation and diffusivity, Mater. Struct. 25 (1992) 523–533.

[20] F. Sanchez, A.C. Garrabrants, C. Vandecasteele, P. Moskowicz, D.S. Kosson, Environmental assessment of waste matrices contaminated with arsenic, J. Hazard. Mater. B96 (2003) 229–257.

[21] H.F.W. Taylor, A method for predicting alkali ion concentrations in cement pore solutions, Adv. Cem. Res. 1 (1987) 5–17.

[22] M. Berra, T. Mangialardi, A.E. Paolini, Effect of fly ash on alkali-silica reaction, in: Proc. 9th Int. Conf. on Alkali-Aggregate Reaction in Concrete, London, 27–31 July, 1992, pp. 61–70.

[23] M.A. Bérubé, C. Tremblay, Chemistry of pore solution expressed under high pressure-influence of various parameters and comparison with the hot-water extraction method, in: Proc. 12th Int. Conf. on Alkali-Aggregate Reaction in Concrete, Beijing, 15–19 October, 2004, pp. 833–842.

[24] CRC Handbook of Chemistry and Physics, 73rd ed., CRC Press, London, 1992.

[25] J. Kragten, Atlas of Metal-Ligand Equilibria in Aqueous Solution, Ellis Horwood Ltd., Chichester, 1978.

[26] L.D. Benefield, J.F. Judkins, B.L. Weand, Process Chemistry for Water and Wastewater Treatment, Prentice-Hall Inc., Englewood Cliffs, New Jersey, 1982.